iScience, Volume *24*

Supplemental information

Targeting B cells in the pre-phase of systemic autoimmunity globally interferes with autoimmune pathology

Anja Werner, Simon Schäfer, Olga Zaytseva, Heike Albert, Anja Lux, Jasminka Krištić, Marija Pezer, Gordan Lauc, Thomas Winkler, and Falk Nimmerjahn

Figure S1

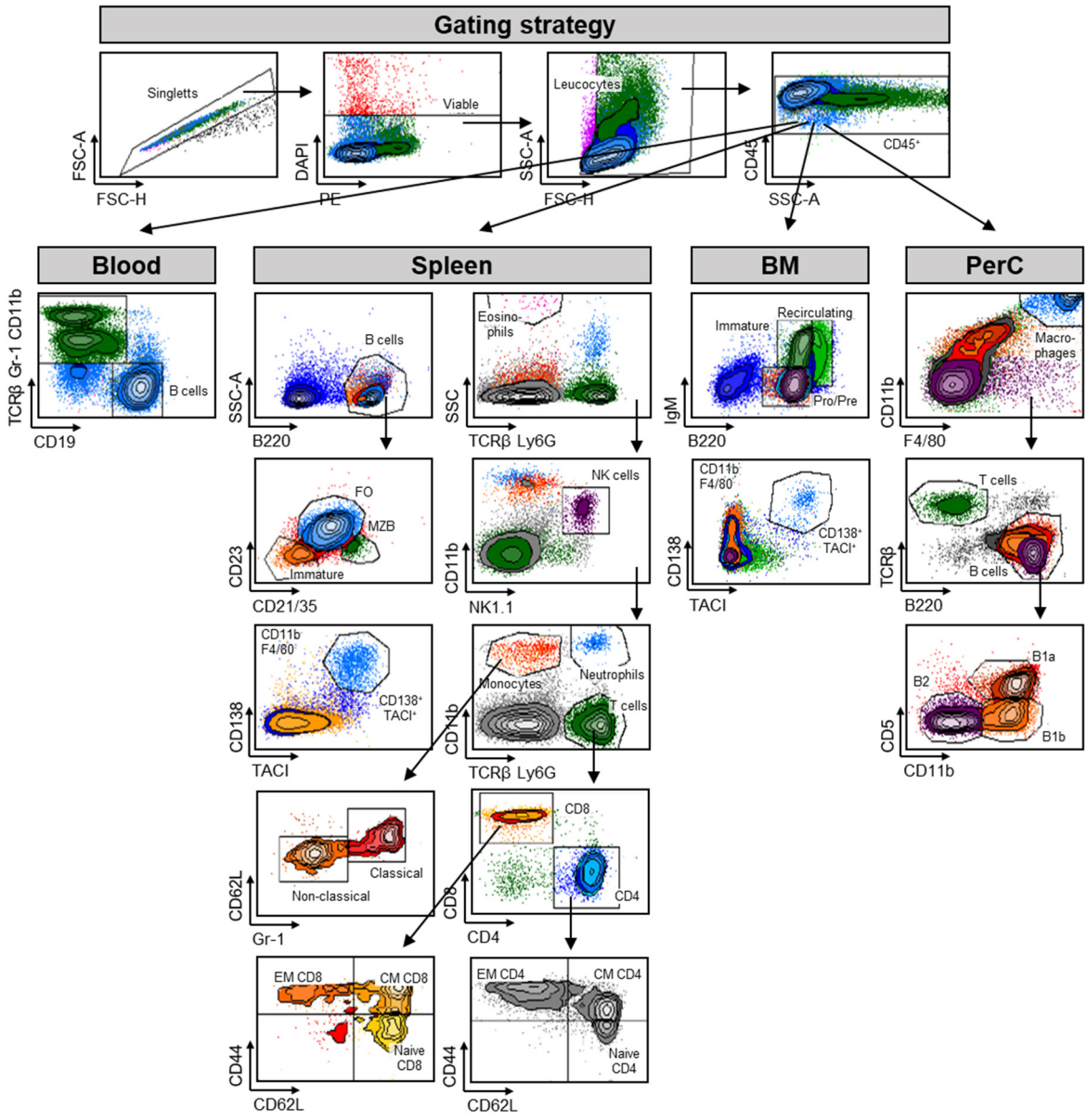

Figure S1: Gating strategy for flow cytometry analysis of immune cells in BXSB mice. Shown are representative FACS plots of single cell suspensions of $CD45^+$ cells in blood, spleen, bone marrow (BM) and peritoneal cavity (PerC). The antibody panels and the gating strategy for identifying the different immune cell populations are depicted. Arrows mark consecutive gating events. FO: follicular B cells, MZB: marginal zone B cells, EM: effector memory, CM: central memory.

Figure S2

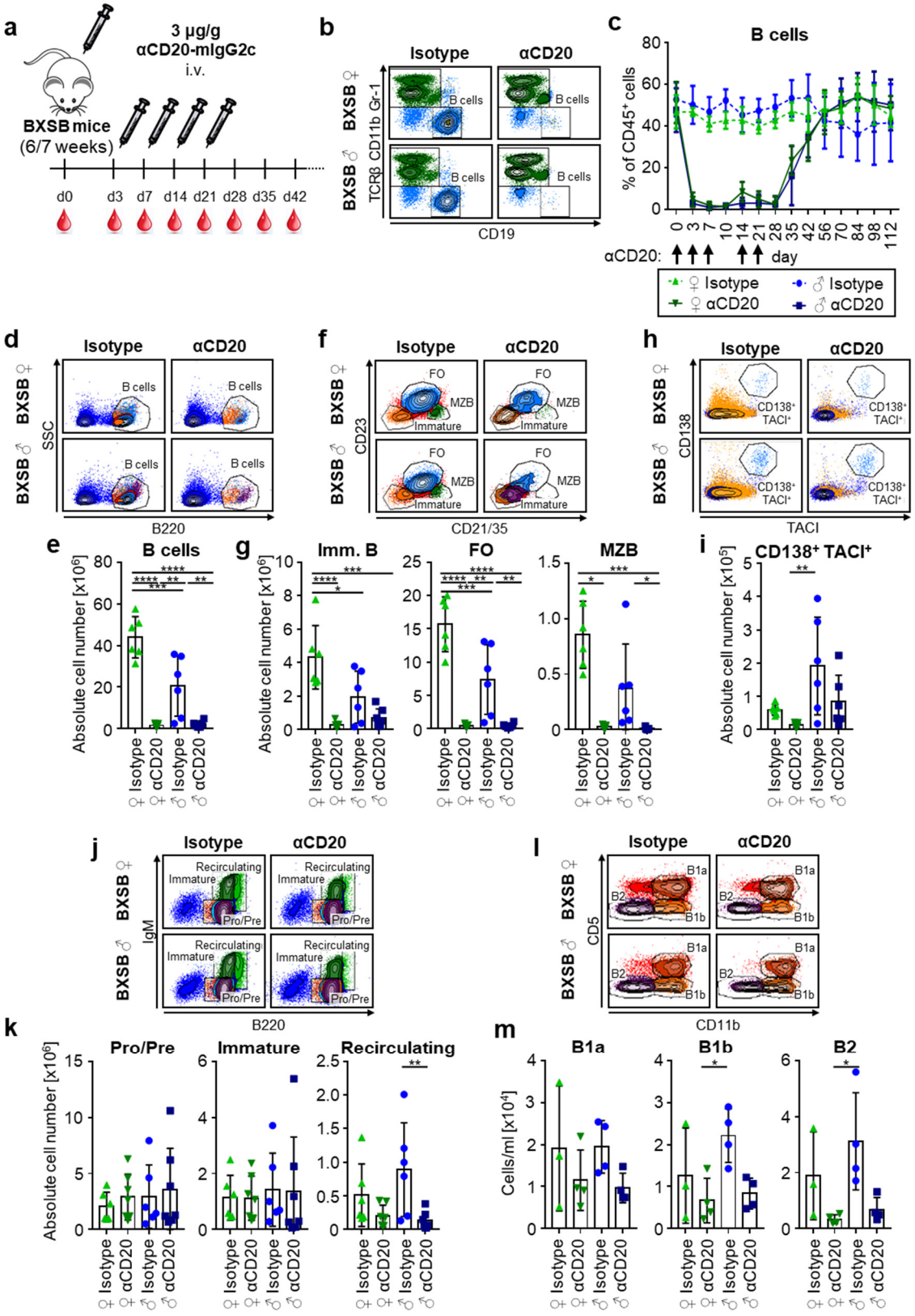

Figure S2: Effect of short-term B cell depletion on B cell subsets in BXSB mice.

(a) Experimental strategy for depletion of B cells during the pre-phase of disease. Time points for CD20-specific antibody injection and collection of peripheral blood are indicated above or below the time scale, respectively.

(b, c) Shown are representative FACS plots identifying peripheral blood B cells (b) and the quantification (c) of B cells over time in the peripheral blood of female (♀) and male (♂) BXSB mice receiving an isotype control or anti-CD20 (αCD20) antibody. Arrows indicate time points of anti-CD20 antibody treatment. Depicted are three independent experiments with n=9-12 mice per group.

(d-i) Depicted are representative FACS plots identifying all splenic B cells (d) or B cell subpopulations (f, h) and the quantification of all B cells (e), immature (Imm. B), follicular (FO) and marginal zone (MZ) B cells (g) and $CD138^{+}$ $TACI^{+}$ plasma blasts and plasma cells (i) four days after initiation of treatment with isotype control or CD20-specific antibodies of female (♀) and male (♂) BXSB mice. Shown are two independent experiments with n=6-7 mice per group.

(j, k) Shown are representative FACS plots identifying pro/pre-, immature-, and recirculating mature-B cell subsets in the bone marrow (j) and the quantification (k) of these B cell subpopulations in female (♀) and male (♂) BXSB mice four days after initiation of treatment with isotype control or CD20-specific antibodies. Shown are two independent experiments with n=6-7 mice per group.

(l, m) Depicted are representative FACS plots identifying peritoneal B1a, B1b, and B2 B cell subsets (l) and the quantification of peritoneal B cell subpopulations (m) in female (♀) and male (♂) BXSB mice four days after initiation of treatment with isotype or CD20-specific antibodies. Shown are two independent experiments with n=6-7 mice per group.

Significant differences between groups were determined with ordinary one-way ANOVA with Tukey's multiple comparison test (normal distribution) or Kruskal Wallis plus Dunn`s multiple comparison test (no normal distribution). *p<0.05; **p<0.01; ***p<0.001; ****p<0.0001.

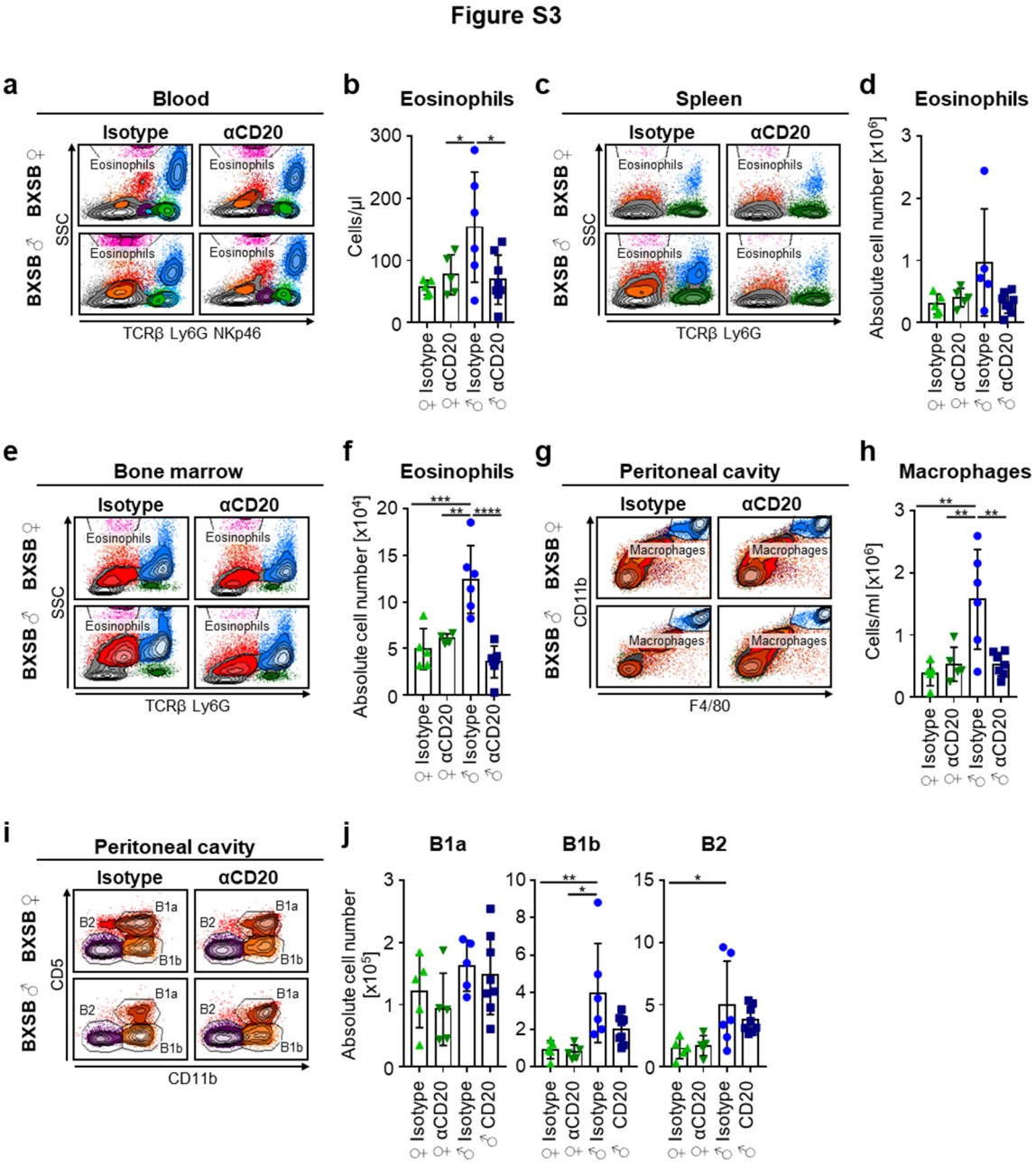

Figure S3: Effect of pre-phase B cell depletion on eosinophils, macrophages, and peritoneal B cell subsets.

(a-f) Shown are representative FACS plots (a, c, e) and the quantification (b, d, f) of blood (a, b), spleen (c, d) and bone marrow (e, f) eosinophils in female (♀) and male (♂) BXSB mice at 18 weeks of age, which were treated with an isotype control or CD20-specific (αCD20) antibody during the pre-phase of disease. Shown are two independent experiments with n=5-7 mice per group.

(h-j) Depicted are representative FACS plots (g, i) and the quantification (h, j) of peritoneal cavity macrophages (g, h) and B cell subsets (i, j) in female (♀) and male (♂) BXSB mice treated with an isotype control or CD20 specific antibody during the pre-phase of disease at 18 weeks of age. Shown are two independent experiments with n=5-7 mice per group

Significant differences between indicated groups were determined with ordinary one-way ANOVA with Tukey's multiple comparison test (normal distribution) or Kruskal Wallis plus Dunn`s multiple comparison test (no normal distribution). *$p<0.05$; **$p<0.01$; ***$p<0.001$; ****$p<0.0001$.

Figure S4

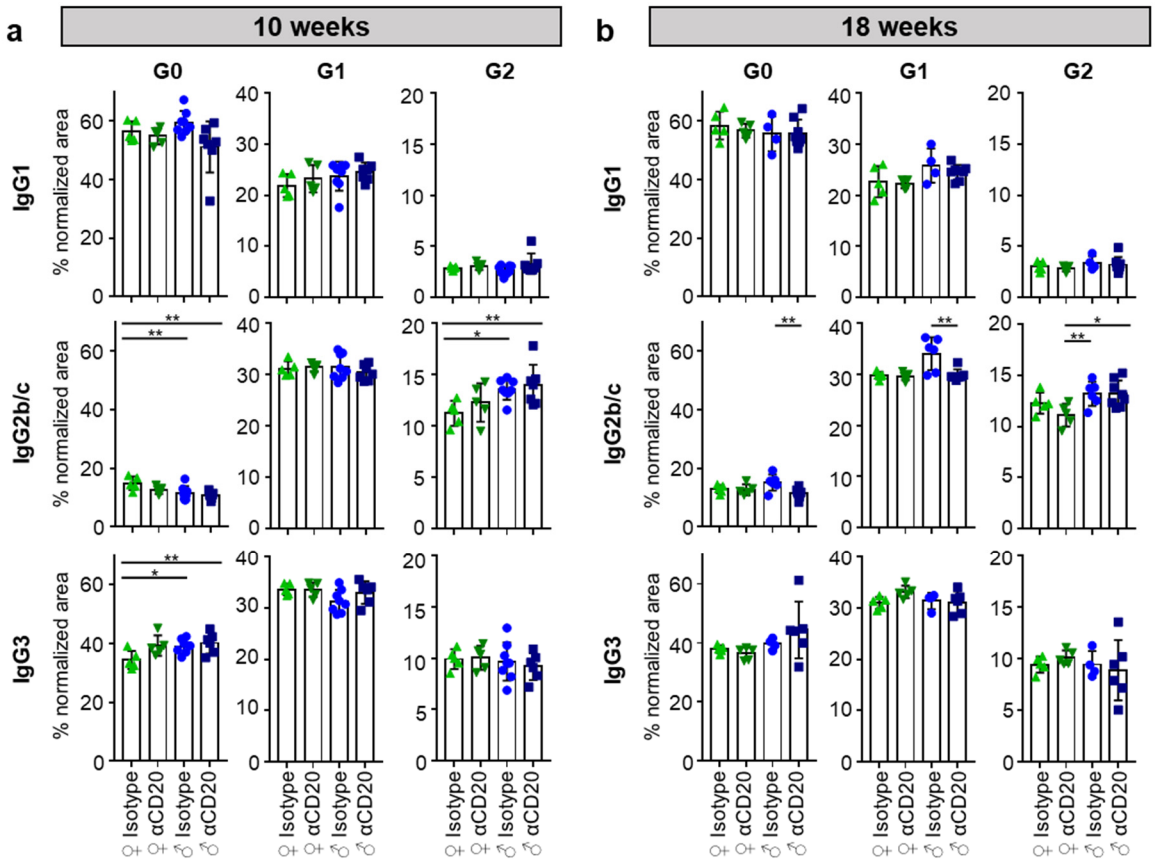

Figure S4: Impact of pre-phase B cell depletion on IgG subclass galactosylation.

Shown is the IgG subclass specific galactosylation pattern in the serum of female (♀) and male (♂) BXSB mice at 10 (a) and 18 weeks (b) of age, which were treated with an isotype control or CD20-specific (αCD20) antibody during the pre-phase of disease. Glycosylation was analysed by Nano-reverse-phase-LC-ESI-MS. Relative abundance (expressed in percent of normalized area) of individual glycan peaks corresponding to agalactosylated (G0), monogalactosylated (G1) and digalactosylated (G2) glycan species was quantified and depicted for the individual subclasses IgG1, IgG2b/c and IgG3. Significant differences between indicated groups were tested with ordinary one-way ANOVA (normal distribution) or Kruskal Wallis test (no normal distribution) and corrected for multiple testing by two-stage step-up method of Benjamini, Krieger and Yekutieli with a false discovery rate of 0.05. Two independent experiments with a total of n=5-7. *$p<0.05$; **$p<0.01$.

Figure S5

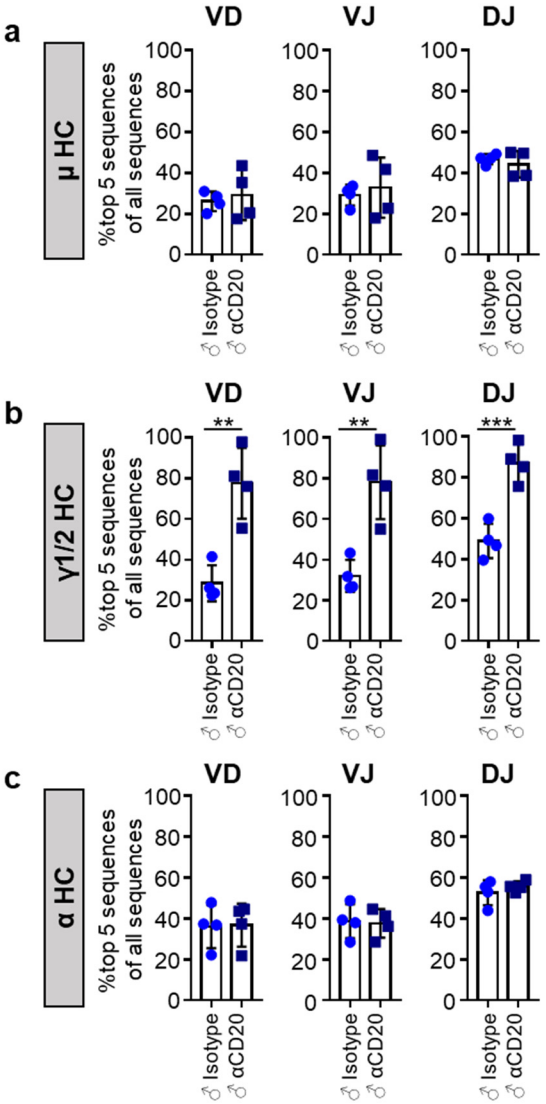

Figure S5: VDJ recombination of heavy chains of anti-CD20 antibody treated BXSB mice

Shown is the percentage of the five most widely used VD, VJ and DJ recombination of all unique productive sequences for each individual mouse in μ (a), γ1/2 (b) and α (c) heavy chains (HC) in splenic cells of anti-CD20 (αCD20) or isotype control antibody treated male (♂) mice at the age of 18 weeks determined by high-throughput RNA sequencing. Bars represent mean ± SD. One independent experiment with a total of n=4 mice. Differences between groups were assessed by Mann-Whitney U test, two-tailed. **p<0.01; ***p<0.001.

Figure S6

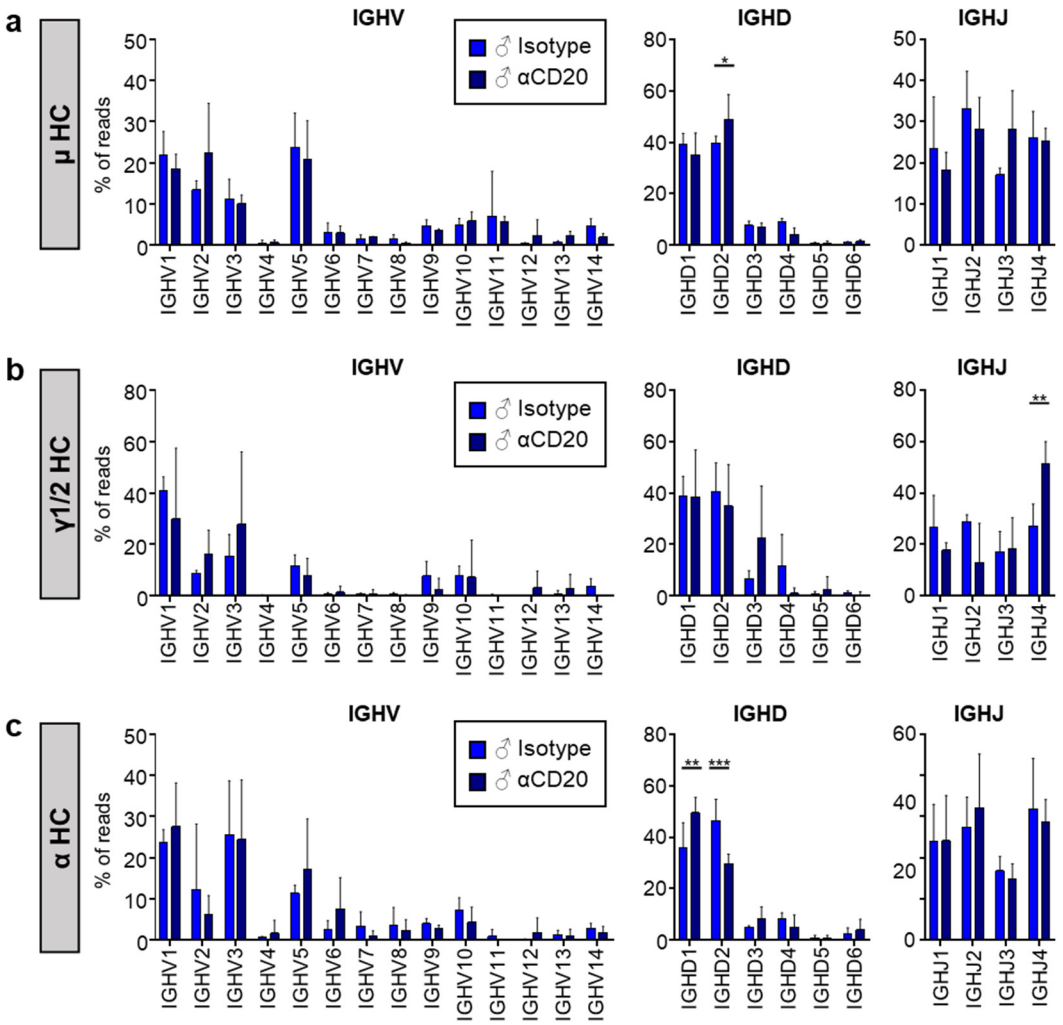

Figure S6: V, D, and J gene segment usage in antibody heavy chains of anti-CD20 antibody treated BXSB mice.

Shown is the abundance (in percent of total reads) of the indicated V (IGHV), D (IGHD) and J (IGHJ) gene segments in μ (a), γ1/2 (b) and α (c) heavy chains (HC) in splenic cells of male (♂) BXSB mice at 18 weeks of age, which were treated with an isotype control or CD20-specific (αCD20) antibody during the pre-phase of disease as determined by high-throughput RNA sequencing. Bars represent mean ± SD. One independent experiment with a total of n=4. Significant differences between groups were determined with an ordinary two-way ANOVA with Sidak's multiple comparison test. *p<0.05; **p<0.01; ***p<0.001.

Figure S7

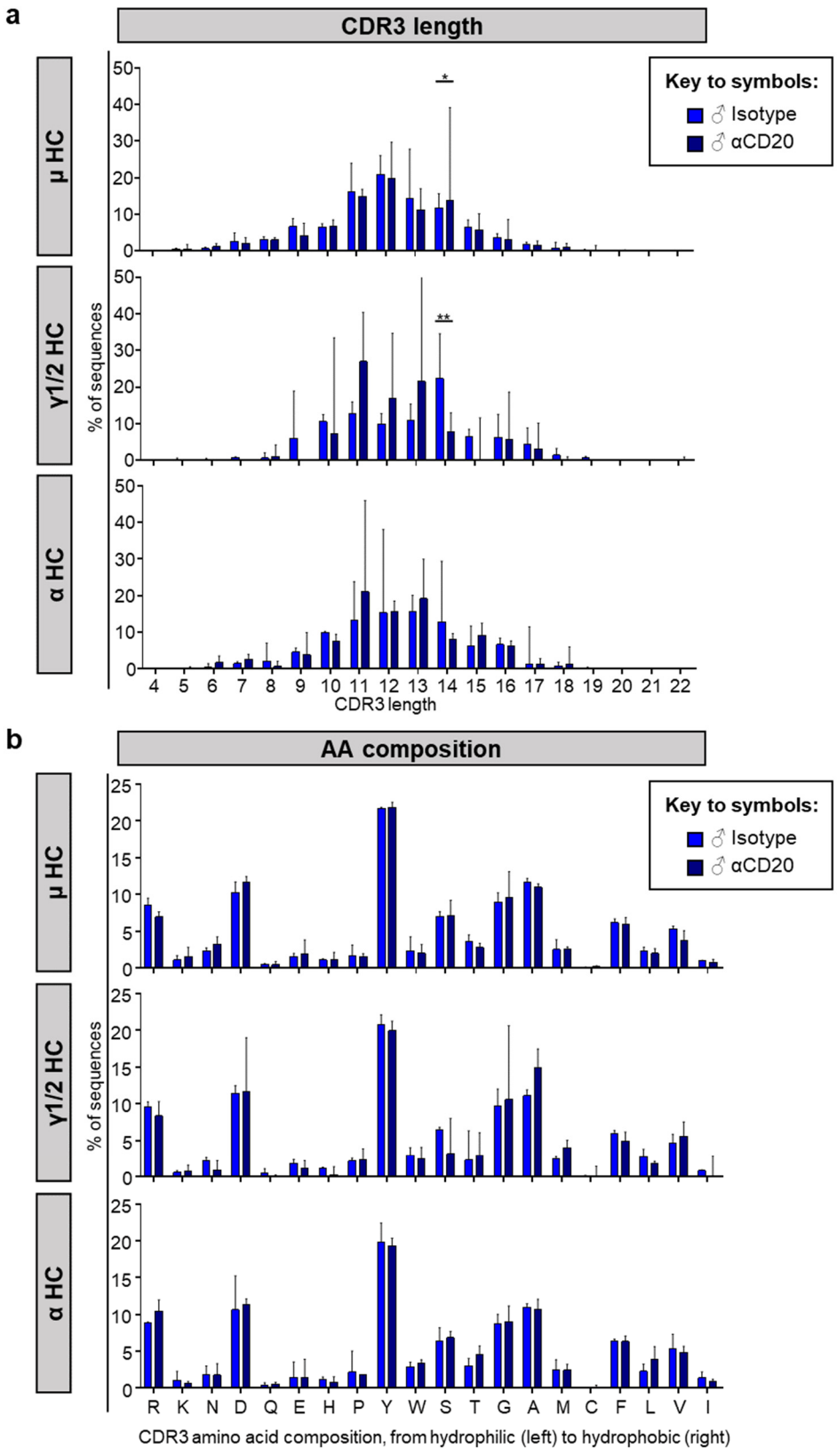
a
CDR3 length
μ HC
γ1/2 HC
α HC
% of sequences
Key to symbols:
♂ Isotype
♂ αCD20
*
**
CDR3 length
b
AA composition
R K N D Q E H P Y W S T G A M C F L V I
CDR3 amino acid composition, from hydrophilic (left) to hydrophobic (right)

Figure S7: Effect of B cell depletion on length and amino acid composition of IgM, IgG and IgM heavy chain CDR3 regions

Analysis of CDR3 regions of μ, γ1/2 and α heavy chains (HC) of male (♂) BXSB mice at 18 weeks of age, which were treated with an isotype control or CD20-specific (αCD20) antibody during the pre-phase of disease. Individual CDR3 length distribution (a) and individual amino acids in the CDR3 region (b) are shown for respective groups. Bars represent mean ± SD. One independent experiment with a total of n=4. Significant differences between isotype and αCD20 treated males for each CDR3 length or amino acid were determined with ordinary two-way ANOVA with Sidak's multiple comparison test. *$p<0.05$; **$p<0.01$.

Figure S8

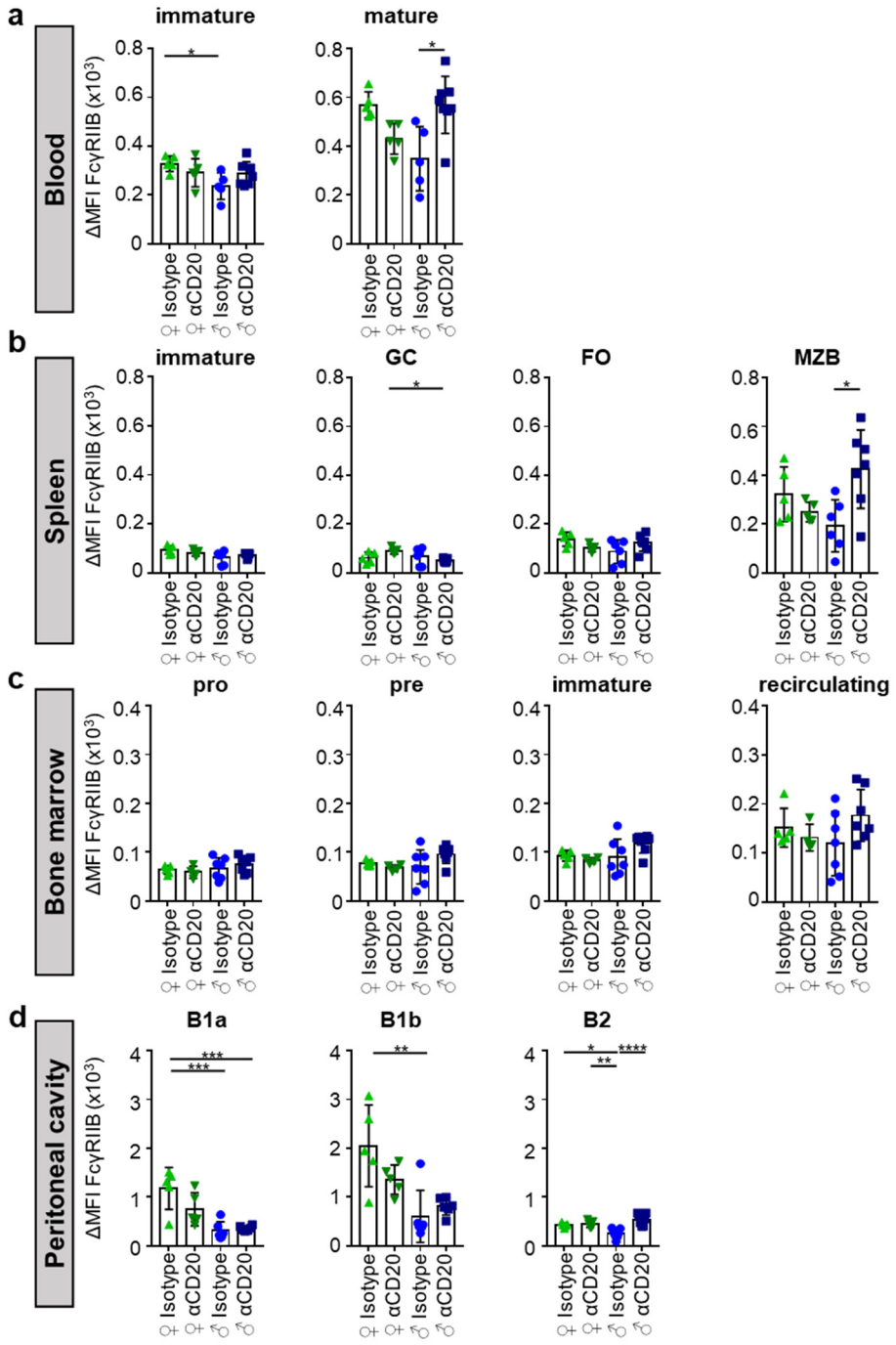

Figure S8: Effect of B cell depletion on FcγRIIB expression on B cell subsets

Analysis of FcγRIIB expression on immature and mature B cell subsets in blood (a), immature, germinal centre (GC), follicular (FO), and marginal zone B cells (MZB) in the spleen (b), pro-, pre-, immature and recirculating B cells in the bone marrow (c), and B1a, B1b, and B2 B cells

in the peritoneal cavity by FACS analysis. Shown are two independent experiments. n=5-7. Significant differences between indicated groups were tested with ordinary one-way ANOVA with Tukey's multiple comparison test (normal distribution) or Kruskal Wallis plus Dunn`s multiple comparison test (no normal distribution). *$p<0.05$; **$p<0.01$; ***$p<0.001$; ****$p<0.0001$.

Figure S9

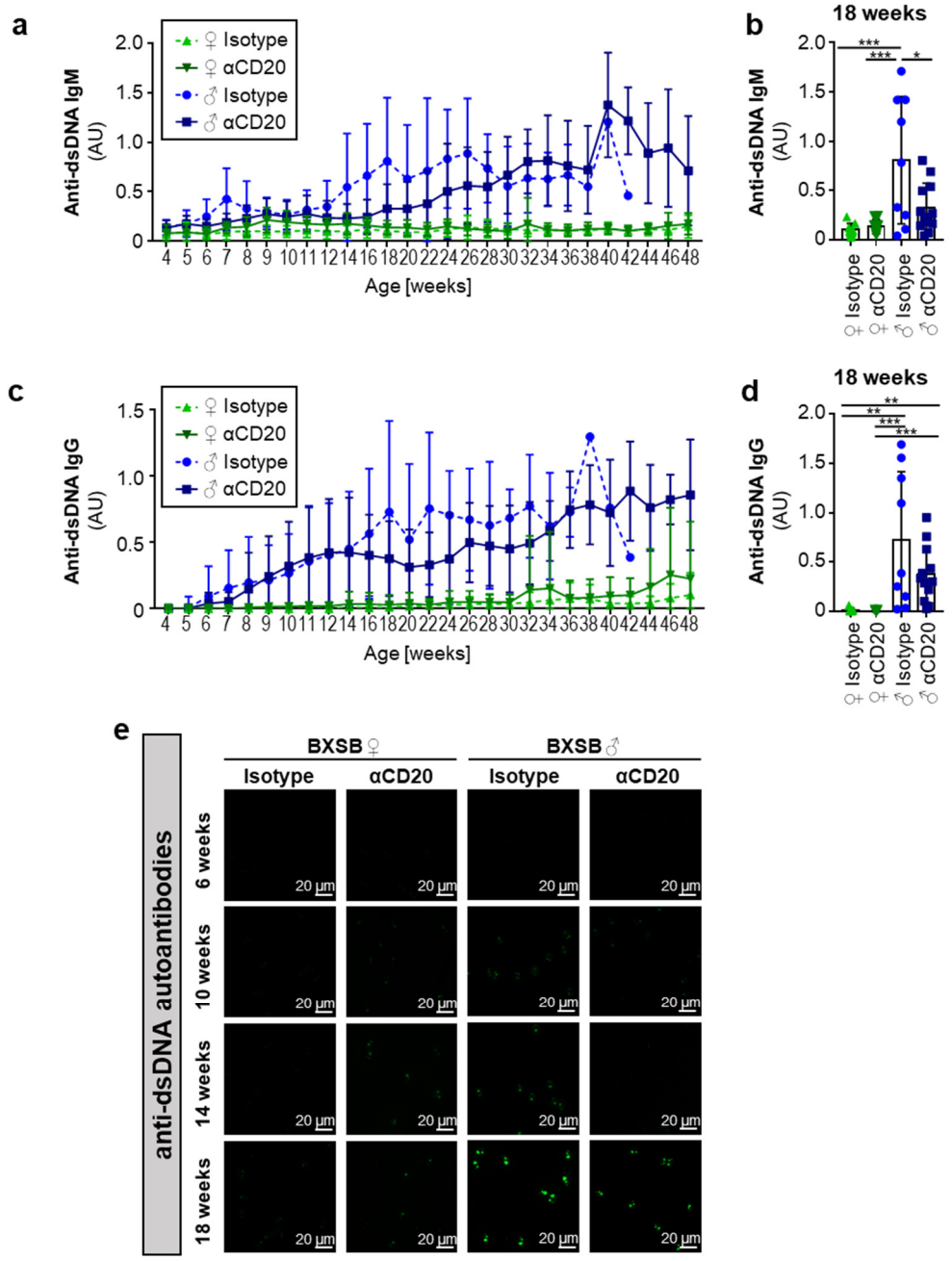

Figure S9: Effect of SLE pre-phase B cell depletion on the production of anti-dsDNA antibodies.

(a-d) Shown is the time course (a, c) and the quantification at the age of 18 weeks (b, d) of anti-dsDNA IgM (a, b) and IgG (c, d) autoantibody production in arbitrary units (AU) in the serum of isotype or anti-CD20-mIgG2c (αCD20) treated female (♀) and male (♂) BXSB mice as

determined by ELISA. Bars represent mean ± SD. Shown are three independent experiments. n=9-12. Significant differences between indicated groups were tested with ordinary one-way ANOVA with Tukey's multiple comparison test (normal distribution) or Kruskal Wallis plus Dunn`s multiple comparison test (no normal distribution). *$p<0.05$; **$p<0.01$; ***$p<0.001$.

(e) Production of anti-dsDNA IgG autoantibodies in the serum of isotype or anti-CD20-mIgG2c (αCD20) treated female (♀) and male (♂) BXSB mice was identified by Crithidia lucilia indirect immunofluorescence test at the indicated time points.. Size bars indicate 20 µm. Representative pictures are shown.

Figure S10

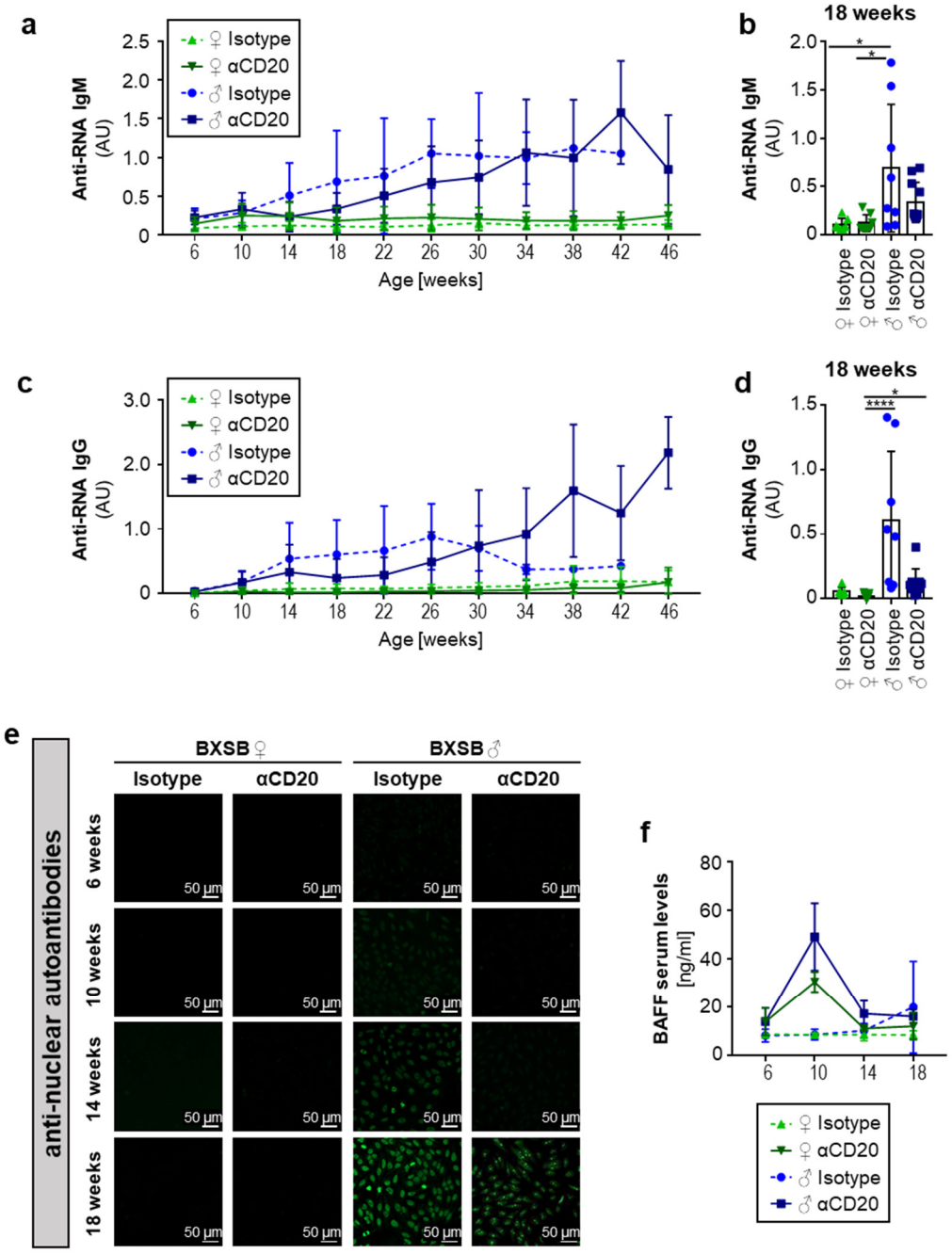

Figure S10: Effect of SLE pre-phase B cell depletion on the production of anti-RNA antibodies, anti-nuclear antigen specific antibodies and serum BAFF levels.

(a-d) Shown is the time course (a, c) and the quantification at the age of 18 weeks (b, d) of anti-RNA IgM (a, b) and IgG (c, d) autoantibody production in arbitrary units (AU) in the serum of isotype or anti-CD20-mIgG2c (αCD20) treated female (♀) and male (♂) BXSB mice as

determined by ELISA. Bars represent mean ± SD. Shown are three independent experiments. n=9-12. Significant differences between indicated groups were tested with Kruskal Wallis plus Dunn`s multiple comparison test. *p<0.05; ****p<0.0001.

(e) Identification of anti-nuclear antibodies in the serum of isotype or anti-CD20-mIgG2c (αCD20) treated female (♀) and male (♂) BXSB mice via HEpG2 cell immunofluorescence at the indicated time points. Size bars indicate 50 µm. Representative pictures are shown.

(f) BAFF serum levels of isotype or anti-CD20-mIgG2c (αCD20) treated female (♀) and male (♂) BXSB mice were determined at the indicated time points by ELISA. Shown are two independent experiments. n=4.

Supplemental Table 1

TABLE I: Number of **unique productive** reads per sample

sample	μ HC	γ1/2 HC	α HC
♂ Isotype #1	52.494	8.187	233.908
♂ Isotype #2	259.373	32.299	277.826
♂ Isotype #3	295.270	72.918	330.628
♂ Isotype #4	57.226	28.001	301.302
♂ αCD20 #5	24.352	774	9.917
♂ αCD20 #6	35.788	3.527	18.431
♂ αCD20 #7	41.002	509	18.487
♂ αCD20 #8	57.848	1.728	26.280

TABLE I: Number of **total** reads per sample

sample	μ HC	γ1/2 HC	α HC
♂ Isotype #1	53.962	8.414	235.394
♂ Isotype #2	262.874	32.468	279.841
♂ Isotype #3	301.784	73.548	333.312
♂ Isotype #4	57.226	28.001	301.302
♂ αCD20 #5	24.772	778	9.988
♂ αCD20 #6	36.778	3.590	18.611
♂ αCD20 #7	42.205	510	18.547
♂ αCD20 #8	59.288	1.737	26.456